WIND TUNNEL SIMULATION OF STRATIFIED ATMOSPHERIC BOUNDARY LAYERS FOR STUDIES OF URBAN DISPERSION

Davide Marucci

EnFlo, Dept. of Mechanical Engineering Sciences
University of Surrey
Guildford, GU2 7XH, UK
d.marucci@surrey.ac.uk

Matteo Carpentieri

EnFlo, Dept. of Mechanical Engineering Sciences
University of Surrey
Guildford, GU2 7XH, UK
m.carpentieri@surrey.ac.uk

ABSTRACT

Moderately stable and convective boundary layers have been investigated in a large environmental wind tunnel. Artificial thickening has been employed by means of "spires" at the inlet section together with densely arranged roughness elements on the floor in order to reproduce conditions suitable for urban-like boundary layer studies. Temperature profiles in the wind tunnel were adjusted by using heaters and cooling panels in several locations. By comparison with lower-roughness cases, roughness does not seem to affect thermal turbulent quantities in the investigated range of stability/instability. For the convective boundary layer simulation, a proper calibrated capping inversion was found to greatly enhance the lateral uniformity.

INTRODUCTION

Atmospheric stratification is due to differences in air density caused by a positive (stable) or negative (unstable) vertical gradient of virtual potential temperature. Stability affects the atmospheric boundary layer (ABL) depth and structure as well as velocity, temperature and turbulence profiles within it. Stratified conditions are frequently present in environmental flows: Argyle & Watson (2012) data analysis demonstrates that non-neutral atmospheric stratification is present 70% of the time for two UK offshore wind farm sites. Nevertheless, most of the studies focus only on neutral flows due to the difficulties on studying atmospheric stratification both experimentally and numerically.

A number of wind tunnel experiments involving stratified BLs have been reported so far. Among them, Ohya & Uchida (2008), Hancock & Pascheke (2014) and Hancock & Hayden (2016) involve stable stratification (SBL), while Fedorovich & Kaiser (1998), Ohya & Uchida (2004) and Hancock *et al.* (2013) deal with convective boundary layers (CBL). Although artificial thickening techniques for the BL (Irwin, 1981) are widely employed for neutral stratification, only Hancock's studies attempted to use them to simulate stratified flows. Nevertheless, their usage is advisable in order to make the boundary layer growing faster and to match the scale of the model (e.g. an array of buildings).

A method to simulate artificially thickened SBL, at least for moderate stability levels and no overlying inversion, has been developed in the EnFlo thermally stratified wind tunnel (Hancock & Hayden, 2016) for offshore low-roughness ABLs. The method has been successfully applied in the present study for high-roughness urban-like conditions: results will be discussed with particular focus on the inlet conditions.

An artificially thickened CBL has also been investigated. In this case great efforts were put on the enhancement of longitudinal and lateral uniformity of the temperature and velocity fields. In particular, the use of different inlet temperature gradients as well as an overlying inversion have been tested for this purpose.

The methodologies developed here will be employed in pollution disperion studies in urban-like arrays of buildings under stratified conditions, where the BLs here described will constitute the approaching flow to the model.

METHODOLOGY

Flow measurements were performed in the suck-down open-return EnFlo meteorological wind tunnel, whose test section was 20 m long, 3.5 m wide and 1.5 m high. The x-axis was in the streamwise direction, measured from the working-section inlet; the y-axis was in the lateral direction, measured from the wind tunnel centre line; the z-axis represented the vertical, starting from the floor. The wind tunnel flow speed could range from 0.3 to 2.5 m/s as measured by a sonic anemometer placed at $x = 5$ m, $y = 1$ m, $z = 1$ m (which provided a reference velocity U_{REF}).

The wind tunnel was specifically designed to generate stratified flows: a series of 15 vertically piled electrical heaters at the inlet section allowed the generation of a vertical temperature gradient, which combined with the heating/cooling floor system created the different types of atmospheric stabilities. For stable stratification the central 3 m of the floor were cooled by means of recirculating water and the desired temperature obtained adjusting the temperature of the water itself. When CBLs had to be simulated, electrical heater mats were added on the wind tunnel floor (on top of additional insulating panels). Their maximum power was 2.0 kW/m^2, with dimensions $1295\times333\times5$ mm; different arrangements were considered in order to improve the lateral uniformity (further explanation will be given in the following sections). Panel temperatures were controlled in a closed-loop control system. The air leaving the wind tunnel was cooled by means of recirculating water in order to keep the laboratory temperature as constant as possible. The latter presented a vertical variation up to $1^{\circ}C$ between floor and ceiling. Such a gradient was mitigated using a series of fans that helped air mixing, improving the temperature homogeneity at the inlet.

Irwin-like spires (Irwin, 1981) after the inlet section and rectangular-shaped roughness elements on the floor were employed to artificially develop the flow. For the CBL simulation five spires 1260 mm high, 170 mm wide at the base and spaced laterally 630 mm were used. They had been extensively employed in previous works for generating urban neutrally stratified BLs about 1 m thick, together with surface roughness elements 80 mm wide, 20 mm high and 2 mm thick placed on the floor in a staggered arrangement with both streamwise and lateral pitches of 240 mm. For the stable stratification case a shallower BL was required for scaling issues: in fact in the real atmosphere a SBL tends to be shallower than a NBL or a CBL. Moreover, a shallower BL would allow us to move the measurement traverse to locations outside the BL (the measuring traverse system is currently limited to a maximum height of about 1 m). For this purpose seven spires 986 mm high, 121 mm wide at the base, and 4 mm wide at the top, spaced laterally 500 mm, were designed according to Irwin's procedure (Irwin, 1981). For all the investigated cases the same roughness element type and arrangement was employed.

Mean and fluctuating velocity measurements were performed by a two-component laser-Doppler anemometer (LDA), via a Dantec 27 *mm* FibreFlow probe. For the fluctuating temperature measurements a calibrated fast-response cold-wire probe was used. It was placed about 3.5 *mm* downstream the LDA measuring volume to calculate heat fluxes. This value was chosen in order to reduce the blockage effect of the cold-wire on the measured flow velocity without affecting dramatically the correlation between velocity and temperature (see Hancock *et al.*, 2013; Heist & Castro, 1998). A thermistor was held about 10 *mm* on the side of the cold-wire to both measure the mean temperature and calibrate the cold-wire itself. The probes were held by a traverse system mounted on rails on the wind tunnel ceiling, which allowed full three-dimensional movements, ranging from about 6 to 16 *m* along x, -1 to 1 *m* on y and from 0.05 to 1.0 *m* on z. In order to measure mean temperatures above such a height during the CBL simulation, a second thermistor was placed 430 *mm* above the LDA measuring volume. Moreover, a double thermistor rake made up of two series of 16 sensors each was employed in the CBL study in order to acquire the temperature field in the section (600 *mm* downstream the LDA measuring volume). It spanned from 50 *mm* to 1350 *mm* of height and its acquisition rate was 0.5 Hz. The sampling rate target for the LDA was set to be around 100 Hz, 1000 Hz for the cold-wire, but with a low-pass filter at 250 Hz. The sampling time for the measurements was 3 minutes both in the SBL and NBL tests, while it was increased up to 5 minutes for the CBL. In the latter, an even longer period was advised based on the scatter between sets of profiles, but this would have increased the experiments duration too much. Data acquisition was performed with the standard Labview based software system of the laboratory.

STABLE BOUNDARY LAYER: RESULTS

Firstly, a review of the effect of the main temperature control parameters is reported. Then, cases of SBLs with moderate stability will be analysed in more details through a comparison with NBL data and field measurements.

Temperature controls

In order to simulate a SBL in the EnFlo wind tunnel, three temperature settings are important: the maximum temperature difference $\Delta\Theta_{MAX}$ between cooled floor Θ_0 and free stream flow Θ_∞, the length of uncooled floor between the inlet and cooled part, and the imposed temperature profile at the inlet section up to the BL height. A forth temperature parameter would be the gradient of temperature imposed above the BL, if an overlying inversion were considered. However, as already mentioned, only zero-strength overlying inversion cases were analysed in order to reduce the number of parameters. In the present study, since only moderate stability cases were supposed to be investigated, a fixed $\Delta\Theta_{MAX}$ of $16^\circ C$ was imposed. The level of stability can also be varied by changing the flow velocity and so allowing the air to be cooled by the floor for a different amount of time.

The second parameter to be considered is the length of uncooled floor after the inlet. Previous studies conducted in the EnFlo laboratory for offshore BL (Hancock & Hayden, 2016) found a dependency of the Reynolds shear stress $\overline{uw}$ profile from this parameter. Investigating different uncooled floor lengths, the best result for the longitudinal uniformity was found with 5 *m* for both the offshore BL and the high-roughness case presented here. More in general, the length of uncooled floor has to be chosen accordingly to the inlet temperature profile.

Finally, a proper inlet temperature gradient has to be considered. The easiest solution would be to impose a uniform inlet temperature and allow the stability to grow thanks to the cooling effect of the floor. However, Hancock & Hayden (2016) found that with this configuration the upper part of the layer remained unaffected by stability: constant vertical mean temperature, while temperature fluctuation and heat fluxes approached zero lower than how the Reynolds shear stress showed. This behaviour was likely caused by the advection downstream of the uniform temperature at the inlet (increased by the reduced level of turbulence). On the other hand, also a near constant inlet temperature gradient does not seem to be the best choice. This option was investigated by Ohya & Uchida (2003) and Hancock & Pascheke (2014) and the resulting BL presented decreasing temperature fluctuations with height z, followed by a rise in the middle region which was attributed by the authors to a too large gradient of mean temperature in the same region. More promising is the approach experimented by Hancock & Hayden (2016). The idea was to impose the measured profile in a naturally-growing SBL (where "naturally-growing" is referred to a BL created just by friction with the cooled floor, without any flow generator or roughness element) as inlet temperature profile, starting from an initial uniform profile. The acquired temperature profile was stretched to fit the desired $\Delta\Theta_{MAX}$ and BL height h and applied to the inlet section with flow generators and roughness elements in place again. The resulting profile is shown in Figure 1a and referred as "Natural".

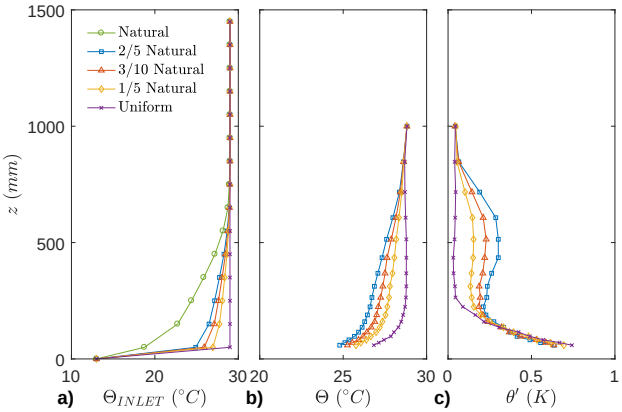

Figure 1. Effect of variation of inlet temperature profile gradient (a) on mean (b) and fluctuating (c) temperature profiles at $x = 6480\ mm$. $U_{REF} = 1.50\ m/s$

However, a direct application of such an initial condition created a large peak in the middle region of the temperature fluctuation graph (not repeated here since it would have required a temperature in the bottom part of the profile lower than the laboratory temperature). Hence, the original gradient was reduced applying corrective factors until the best solution was found. The other cases in Figure 1 represent respectively a reduction of a factor 2/5, 3/10, 1/5 of the "natural" one; also the uniform temperature case is shown. They were acquired after just 1.5 *m* of floor cooling, and so still in the developing region of the flow. The major effect of varying the inlet gradient is on the temperature fluctuation; in fact, even though the temperature standard deviation profiles show the same trend in the bottom part (Figure 1c) a peak is present in the middle region for the 2/5 case (and it would be even worse approaching the "natural" gradient). The peak is quite reduced for the 3/10 case and disappeared for the 1/5 and the uniform profile. However, in the last one the reduction is so accentuated to generate an almost NBL on top of the stable one, as noted previously. The 3/10-reduced version of the inlet temperature profile was chosen as upstream condition for the

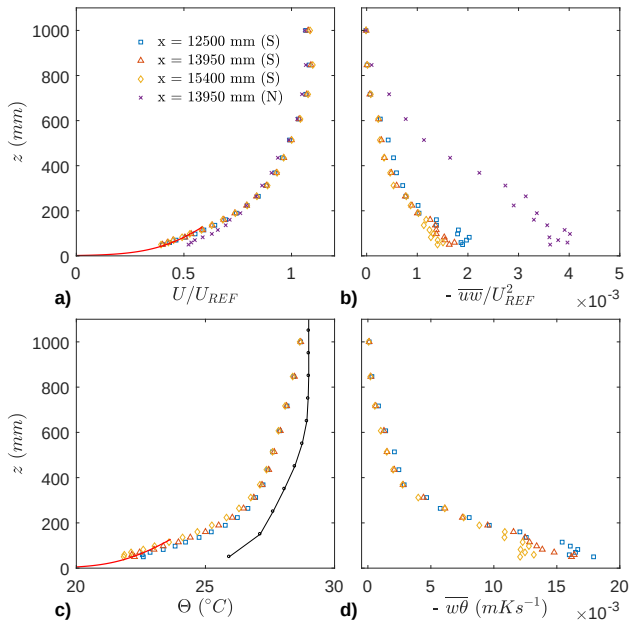

Figure 2. Profiles of mean streamwise velocity, Reynolds shear stress, mean temperature and vertical kinematic heat flux for U_{REF} = 1.25 m/s at the centreline. Red lines in (a) and (c) are Equation 1 and 2, respectively. Black line in (c) is the inlet temperature profile

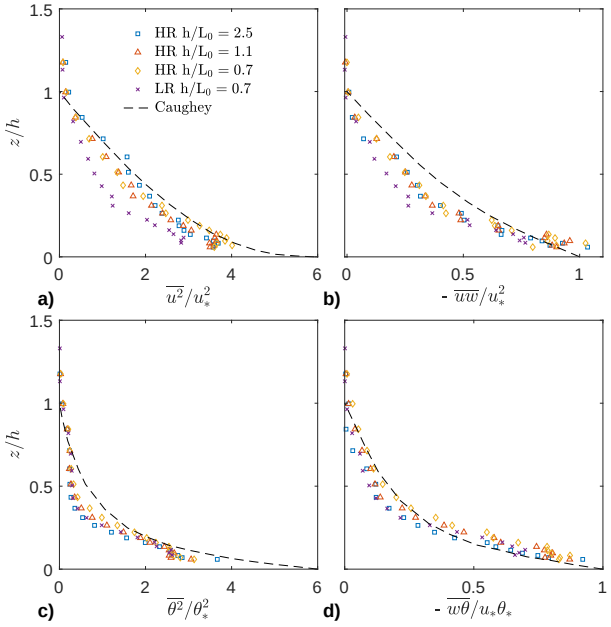

Figure 3. Profiles of non-dimensionalised streamwise velocity variance, Reynolds shear stress, temperature variance and vertical kinematic heat flux for different level of stability and roughness. the low-roughness case (LR) is from Hancock & Hayden (2016) while dashed line is field data from Caughey *et al.* (1979)

other experiments.

Mean and turbulent profiles

Figure 2 shows stable (S) profiles with $U_{REF} = 1.25\ m/s$ at three streamwise locations and a neutral (N) at a single station for comparison. The mean velocity and Reynolds shear stress profiles in Figure 2a and b show an h of approximately 850 mm, equal for stable and neutral stratifications. This allows us to hypothesize that the combination of chosen spires and temperature profile overcomes the effect of stability to reduce h. Moreover, the BL is stable for the entire h, because a temperature gradient is present for all the depth in c) and the heat flux in d) approaches zero only on top of the BL. The reduction of turbulence due to stratification is evident in b) and it carries to a friction velocity $u_* = \sqrt{|(\overline{uw})_0|}$ value 30% lower in the SBL respect to NBL (u_*/U_{REF} = 0.044 and 0.066, respectively; where $(\overline{uw})_0$ was estimated with a linear fitting in the bottom of the Reynolds shear stress profile).

This case is one of weak/moderate surface condition (in terms of Monin-Obukhov length L_0). In fact $h/L_0 \approx 1.2$, where $L_0 = (-1/k)(\Theta_0/g)(u_*^3/(\overline{w\theta}_0))$. $k = 0.40$ is the von Karman constant and $(\overline{w\theta})_0$ the vertical kinematic heat flux at the surface extrapolated as for the friction velocity. The aerodynamic z_0 and thermal z_{0h} roughness lengths were calculated by means of a non-linear fitting of the bottom part of mean velocity and temperature profiles, respectively with Equation 1 and 2 (as shown in Figure 2a and c). Following Dyer (1974); Högström (1988) and Högström (1996), for the surface layer SL

$$U(z) = \frac{u_*}{k}\left[\ln(z/z_0) + 5\frac{z}{L_0}\right] \tag{1}$$

$$\Theta(z) - \Theta_0 = \frac{\theta_*}{k}\left[0.95\ln\left(\frac{z}{z_{0h}}\right) + 8\frac{z - z_{0h}}{L_0}\right] \tag{2}$$

where the temperature scale for the SL $\theta_* = -(\overline{w\theta})_0/u_*$. z_0 appears reduced of about 20% due to the stratification (from 2.1 to 1.6 mm), while z_{0h} is three orders of magnitude smaller ($z_{0h} \approx 0.001\ mm$).

The roughness Reynolds number $Re_* = u_* z_0/\nu$ can be used to evaluate if the flow is fully turbulent and the experiment independent from U_{REF}. Following Snyder & Castro (2002), employing sharp-edged roughness elements (as the ones used here) the minimum limit would be 1, limit fully respected for both neutral and stable case (being 10.9 and 5.3, respectively). A proper Reynolds independence test was not performed due to the difficulties to change velocity without affecting the stability.

Figure 3 presents a comparison between non-dimensional profiles of Reynolds stresses, temperature fluctuations and vertical heat flux for three velocities ($U = 1.0, 1.25, 1.5\ m/s$). All of them were acquired with the same high-roughness (HR) and temperature settings and, despite the change in stability from h/L_0 = 0.7 to 2.5, the shape of the turbulent profiles seems not affected too much. From the comparison between the low-roughness case (LR) in Hancock & Hayden (2016) also the roughness appears to have very little or no influence on the non-dimensionalised thermal quantities (Figure 3c and d). The characteristics exhibited in Figure 3 are comparable with the field observations of Caughey *et al.* (1979).

The lateral uniformity experienced with stable stratification was generally quite good, with a mean velocity variation of the order of 2%.

CONVECTIVE BOUNDARY LAYER: RESULTS

Similarly to the SBL, in order to simulate a CBL the temperature difference $\Delta\Theta_{MAX}$ and the flow velocity are the main ways to control the level of instability. Important inlet parameters to consider, which where found to influence in a certain manner the lateral uniformity, are the inlet temperature profile and the strength of the inversion imposed above the BL. Before considering the effect of this inlet temperature controls some considerations on the floor heater mats have to be discussed. As already mentioned, the lab-

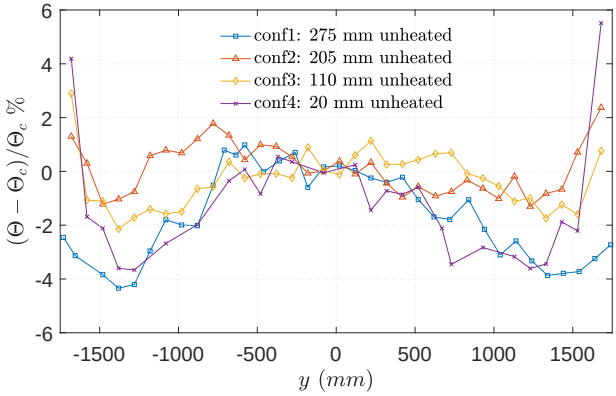

Figure 4. Comparison between different floor heater mats arrangements ($x = 14000$ mm, $z = 300$ mm, $U_{REF} = 1.25$ m/s, $\Delta\Theta_{MAX} \approx 20°C$). Θ_c is the temperature in the centreline

oratory employs 2950 mm long rectangular heater panels, so that placing them transversally on the floor, the last 275 mm on both sides are not heated (being the test section 3.5 m wide). In the past, Perspex panels used to be placed as walls on the sides in order to reduce the test section size, but this remedy was not pursued in this case since the entire wind tunnel width was necessary (for future experiments with the urban model). Therefore four different heater mats arrangements were considered, the first of which consisted in adjacent panels placed transversally, with 275 mm on both sides unheated. In Figure 4 a lateral profile of temperature acquired with the double thermistor rake shows a reduction of up to 4% respect to the centre line (2% in the region ± 1 m). In the other configurations longitudinal panels were added on the sides in order to cover a wider region of the floor[1]. The graph shows that the configuration in which the largest part of the test section is heated does not present the best uniformity, with hot spots closer to the walls, while a reasonable compromise is the third configuration in which 110 mm are left unheated (without the complexity of adjusting the longitudinal panels temperature as for configuration 2).

Temperature controls

For the CBL both an inlet temperature gradient and a capping inversion layer where considered separately. Differently from the SBL, using a NBL as starting point (uniform inlet temperature profile) and obtaining a CBL only by means of the heated floor was found acceptable. This approach was employed, for instance, by Fedorovich & Kaiser (1998) and Ohya & Uchida (2004). Differently, Hancock *et al.* (2013) suggested to adopt as inlet setting the temperature profile measured in a section downstream (starting from a uniform inlet profile) and iterating until a matching of the shape between the two was achieved. This method was tested in the present study with high-roughness conditions with the purpose to enhance the longitudinal uniformity and reduce the wind tunnel length necessary to obtain a sufficiently developed CBL. However, the improvements were generally difficult to appreciate and hard to separate from the experimental scatter. Moreover, applying a negative inlet gradient was found to worsen the lateral uniformity (at least in the presented case). Figure 5 shows the lateral profiles of Reynolds shear stress, temperature variance and mean streamwise velocity for different inlet gradients. Three cases were considered: uniform temperature, "full gradient" from the direct application of the method

[1]In configuraion 2 the longitudinal panel temperature was increased respect to the transversal one until the best uniformity was achieved. In Configurations 3 and 4 all the panels were set at the same temperature

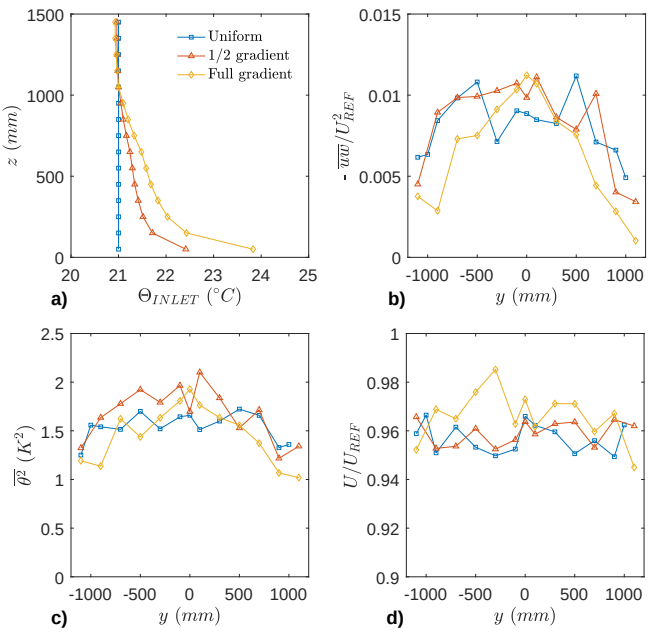

Figure 5. (a) Vertical profile of inlet temperature. Lateral profiles of Reynolds shear stress (b), temperature variance (c) and mean streamwise velocity (d) at $z = 300$ mm ($U_{REF} = 1.0$ m/s, $\Theta_0 = 60°C$, $x = 13900$ mm, floor configuration 4)

and half gradient. The turbulence is less laterally uniform in the "full gradient" case in both the graphs. While the Reynolds shear stress graph shows comparable results for the half gradient and uniform cases, the latter presents a slightly better uniformity in the central region of the temperature variance plot. Interestingly, the non-uniformity due to the gradient affects only turbulent quantities and heat fluxes, while mean velocity (Figure 5d) and temperature profiles (not shown) seem not to be affected.

A capping inversion is a characteristic part of the CBL. In works like Ohya & Uchida (2004) and Fedorovich & Kaiser (1998) great attention was paid to the inversion layer and the entrainment. In the present study the focus was mainly on the simulation of the lower part of the CBL, which is most relevant for flow and dispersion studies in the urban environment. For this reason the correct representation of a capping inversion was not deemed essential. Weak linear inversions were applied above 1 m and with a maximum gradient of $30°C/m$. Inside this range no effects were experienced in the bottom half of the BL. However, a proper calibrated inversion above the BL was found to greatly enhance the lateral uniformity. In Figure 6 the lateral profile of temperature in the upper part with no inversion is compared with two cases with inversions (respectively with a 10 and $20°C/m$ temperature increase). The lateral temperature profile appears colder in the central region respect to the sides. The opposite was found for the $20°C/m$ inversion. On the other hand, employing the $10°C/m$ inversion resulted in a better lateral uniformity of the temperature profiles. This fact seems to suggest that a proper inversion can be defined to match the temperature on the sides with the temperature in the central region. The beneficial effect of such an increased-temperature uniformity can be observed, for example, comparing the vertical profiles of streamwise mean velocity in the centreline with the ones in the sides (Figure 7).

The length of uncooled floor after the inlet did not show the effect noted for the SBL. Only 1 and 4 m were tested and no significant improvements were observed by delaying the heating. 1 m was the length used for all the results shown.

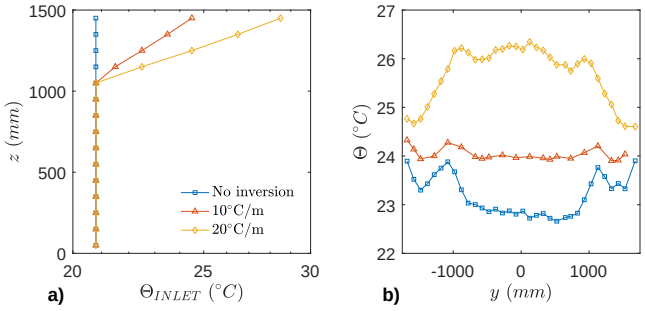

Figure 6. (a) Vertical profile of inlet temperature with different inversion strength. (b) Lateral profiles of temperature acquired with thermistor rake at $z = 1225mm$. ($U_{REF} = 1.0\ m/s$, $\Theta_0 = 60°C$, $x = 14500\ mm$)

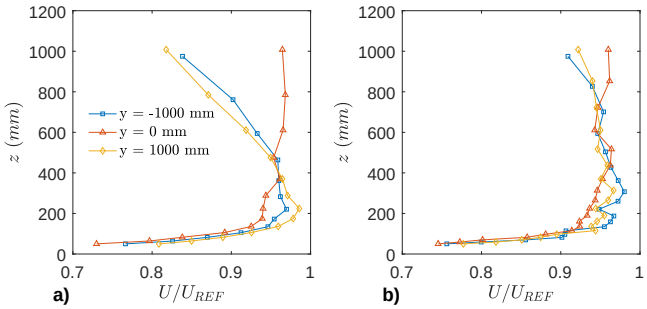

Figure 7. Mean velocity profiles with (a) no inversion and (b) inversion $10°C/m$ at $x = 13900mm$. ($U_{REF} = 1.0\ m/s$, $\Theta_0 = 60°C$)

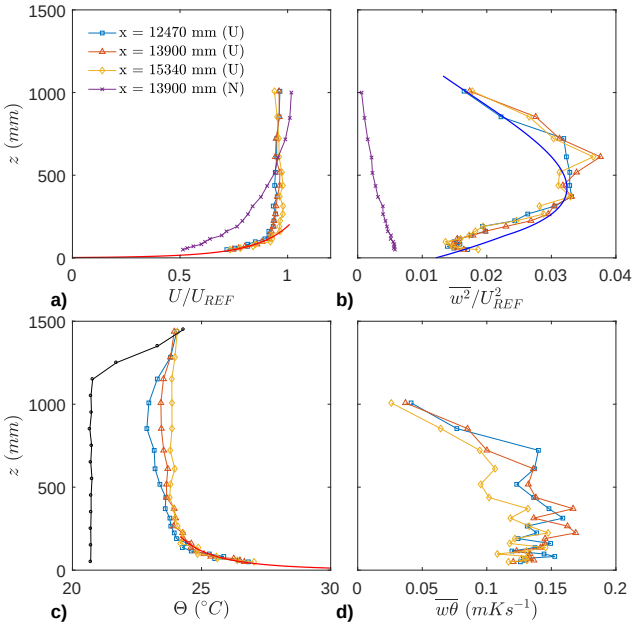

Figure 8. Profiles of mean velocity, vertical velocity variance, mean temperature and vertical kinematic heat flux for a CBL case (U_{REF} = 1.0 m/s and $\Delta\Theta_{MAX} = -36°C/m$) and a reference neutral at the centreline. Red lines in (a) and (c) are Equation 11 and 12 in Hancock *et al.* (2013), respectively. Blue lines in (b) are Equation 3 and 4; black line in (c) is the inlet temperature profile

Mean and turbulent profiles

A CBL case obtained with uniform inlet temperature and an inversion of about $10°C/m$ (adjusted to enhance the lateral uniformity) is presented in Figure 8 and compared with a neutral one. The streamwise mean velocity profile is greatly modify by the stratification: the SL region readily follows the Monin-Obukhov similitude (Equation 11 from Hancock *et al.*, 2013 was used, not reported for brevity), with a sharp "knee" at $z \approx 150\ mm$, while the mixed layer ML above shows constant velocity. The aerodynamic roughness length in this case does not seem to be affected by the different stratification (being 2.0 *mm* for both CBL and NBL), while z_{0h} has a value similar to the SBL previously presented. The mean temperature also follows the similarity in the SL while the inversion appears notably reduced from the value imposed at the inlet, likely due to mixing from below. Reynolds stresses have much larger values compared to the neutral case (u_*/U_{REF} is here 0.100 against 0.066). The shape of the $\overline{w^2}$ profile is significantly different, showing a rise with z followed by a decrease, instead of a monotonic reduction. Canonical similarity functions (see e.g. Kaimal & Finnigan, 1994) do not seem to apply for this low instability case ($h/|L_0| \approx 2.0$). Hancock *et al.* (2013) proposed a modified version to take into account the effect of the shear also in the ML. Here their relations for $\overline{w^2}$ are reported for the SL and ML, respectively

$$\frac{\overline{w^2}}{u_*^2} = 1.1^2 \left(1 + 8\frac{z}{|L_0|}\right)^{2/3} \tag{3}$$

$$\frac{\overline{w^2}}{u_*^2} = 6.63 \left(1 + 0.8\frac{h}{|L_0|}\right)^{2/3} \left(\frac{z}{h}\right)^{2/3} \left(1 - 0.8\frac{z}{h}\right)^2 \tag{4}$$

Equation 4, in particular, could be used to estimate the BL depth h by fitting with the $\overline{w^2}$ profile (Figure 8b): the value of 1.3 *m* provides a reasonable fitting. Otherwise, the normal criterion to identify h with the height for which the vertical heat flux experiences a minimum is not practicable in this case, due to limitation in the traverse movement range.

Figure 9 shows the non-dimensionalised Reynolds stresses, temperature fluctuation and vertical heat flux, in which $w_* = [(g/\Theta_0)(\overline{w\theta})_0 h]^{1/3}$ and $\tilde{\theta}_* = (\overline{w\theta})_0/w_*$ are scaling velocity and temperature for the ML. The high-roughness case previously presented (here called HR1) is compared with a second one characterised by the same roughness but weaker instability (HR2), obtained by changing reference speed and floor temperature ($U_{REF} = 1.25\ m/s$ and $\Theta_0 = 45°C$, with $h/L_0 \approx 0.9$). The case U5 from Hancock *et al.* (2013) is also plotted and allows a comparison with a low-roughness case with similar instability (in this run $h/L_0 \approx 1.26$ and $u_*/U_{REF} = 0.055$). The two weakest cases from Ohya & Uchida (2004) are reported as well (E1 is characterised by $h/L_0 = 1.48$ while E2 by 3.11).

The $\overline{u^2}$ graph shows a good agreement between case HR2 and U5, with similar instability but different roughness. The same can be said for the $\overline{w^2}$ profiles. Again for $\overline{u^2}/w_*^2$ case HR1 presents lower values compared with the weaker case HR2, but the same can be said for cases E1 and E2 with increasing instability. As far as non-dimensionalised temperature variance and vertical heat flux are concerned, a good agreement is shown between all the presented experimental cases. Differently, the field data from Caughey & Palmer (1979) differs more or less widely from the experimental profiles. Probable reasons are the differences in the level of instability ($h/L_0 \geq 30$ in Minnesota experiments) and inversion strength.

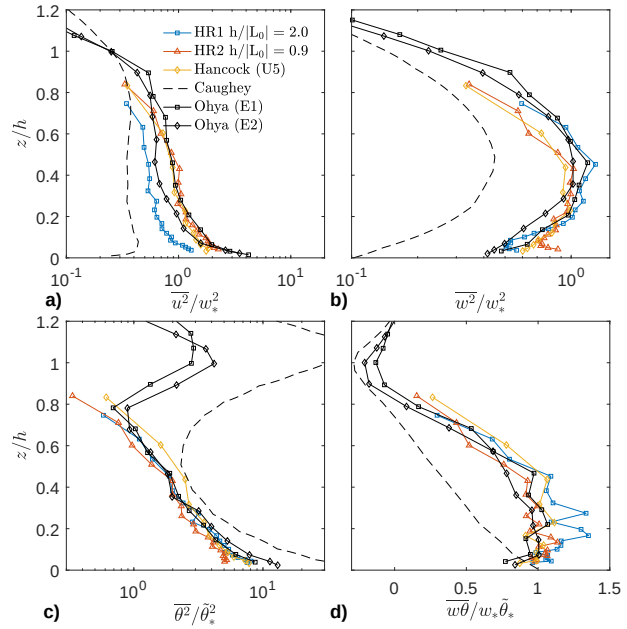

Figure 9. Profiles of non-dimensionalised Reynolds stresses, temperature variance and vertical kinematic heat flux. Yellow line is case U5 from Hancock *et al.* (2013), black continuous lines are cases E1 and E2 from Ohya & Uchida (2004), dashed line is field data from Caughey & Palmer (1979)

CONCLUSION

The methodology presented in Hancock & Hayden (2016) for low-roughness cases has been successfully applied to cases with higher-roughness, suitable for urban-like boundary layers, to reproduce a stable boundary layer in the wind tunnel. The higher roughness gave higher non-dimensionalised Reynolds stresses but very little or no change in the thermal properties. The high-roughness case was in good or reasonable agreement with field measurements (Caughey *et al.*, 1979).

For the simulation of a convective boundary layer great attention was given to the flow uniformity inside the test section. The selection of a non-uniform inlet temperature profile was in this case found not as determinant as for the stable boundary layer to improve the longitudinal uniformity, while the application of a calibrated capping inversion considerably improved the lateral uniformity. The non-dimensionalised vertical profiles of turbulent quantities and heat fluxes, again did not seem to be influenced by roughness (by a comparison with Hancock *et al.*, 2013). Good agreement is also shown with Ohya & Uchida (2004).

The boundary layers presented here will be applied as approaching flow in the following phase to study flow and dispersion in urban-like models under non-neutral stratification.

REFERENCES

Argyle, Peter & Watson, Simon 2012 A study of the surface layer atmospheric stability at two UK offshore sites. In *European wind energy association conference*, pp. 16–19.

Caughey, S. J. & Palmer, S. G. 1979 Some aspects of turbulence structure through the depth of the convective boundary layer. *Quarterly Journal of the Royal Meteorological Society* **105** (446), 811–827.

Caughey, S. J., Wyngaard, J. C. & Kaimal, J. C. 1979 Turbulence in the evolving stable boundary layer. *J. Atmos. Sci.* **36**, 1041–1052.

Dyer, A. J. 1974 A review of flux-profile relationships. *Boundary-Layer Meteorology* **7**, 363–372.

Fedorovich, E. & Kaiser, R. 1998 Wind tunnel model study of turbulence regime in the atmospheric convective boundary layer. In *Buoyant convection in geophysical flows*, pp. 327–370. Springer Netherlands.

Hancock, P E & Hayden, P 2016 Wind-tunnel simulation of stably stratified atmospheric boundary layers. *Journal of Physics: Conference Series* **753** (3), 032012.

Hancock, Philip E. & Pascheke, Frauke 2014 Wind-Tunnel Simulation of the Wake of a Large Wind Turbine in a Stable Boundary Layer. Part 1: The Boundary-Layer Simulation. *Boundary-Layer Meteorology* **151** (1), 3–21.

Hancock, P. E., Zhang, S. & Hayden, P. 2013 A Wind-Tunnel Artificially-Thickened Simulated Weakly Unstable Atmospheric Boundary Layer. *Boundary-Layer Meteorology* **149** (3), 355–380.

Heist, D. K. & Castro, I. P. 1998 Combined laser-doppler and cold wire anemometry for turbulent heat flux measurement. *Experiments in Fluids* **24**, 375–381.

Högström, U. 1988 Nondimensional wind and temperature profiles. *Boundary-Layer Meteorology* **42** (1), 55–78.

Högström, U. 1996 Review of some basic characteristics of the atmospheric surface layer. *Boundary-Layer Meteorology* (January), 215–246.

Irwin, H. P. A. H. 1981 The design of spires for wind simulation. *Journal of Wind Engineering and Industrial Aerodynamics* **7** (3), 361–366.

Kaimal, J C & Finnigan, J J 1994 *Atmospheric boundary layer flows: their structure and measurement*, , vol. 72. Oxford University Press.

Ohya, Yuji & Uchida, Takanori 2003 Turbulence structure of stable boundary layers with a near-linear temperature profile. *Boundary-Layer Meteorology* **108** (1), 19–38.

Ohya, Y. & Uchida, T. 2004 Laboratory and numerical studies of the convective boundary layer capped by a strong inversion. *Boundary-Layer Meteorology* **112**, 223–240.

Ohya, Y. & Uchida, T. 2008 Laboratory and numerical studies of the atmospheric stable boundary layers. *Journal of Wind Engineering and Industrial Aerodynamics* **96** (10-11), 2150–2160.

Snyder, William H. & Castro, Ian P. 2002 The critical Reynolds number for rough-wall boundary layers. *Journal of Wind Engineering and Industrial Aerodynamics* **90** (1), 41–54.